Universitat Autònoma de Barcelona

Human prostaglandin reductase 1 (PTGR1): Substrate specificity, site-directed mutagenesis and catalytic mechanism

Thesis dissertation presented by **Julio Mesa Solís**, in partial fulfillment of the requirements for the degree of Ph.D. in Biochemistry, Molecular Biology and Biomedicine.

The work was performed at the Department of Biochemistry and Molecular Biology in the Universitat Autònoma de Barcelona, under the direction of doctors **Xavier Parés Casasampera, Jaume Farrés Vicén and Sergio Porté Orduna**.

Xavier Parés Casasampera

Jaume Farrés Vicén

Sergio Porté Orduna

Bellaterra, June 9, 2016

4. CHAPTER 3

Carbon-carbon double-bond hydrogenation of 15-deoxy-$\Delta^{12,14}$-prostaglandin J_2 by human prostaglandin reductase 1: Product identification by ^{1}H and ^{13}C NMR spectroscopy and catalytic mechanism

Some of the results of this chapter will appear in the publication:

Mesa J, Porté S, Cabañas M, Jaime C, Parés X, Virgili A, Farrés J. **Carbon-carbon double-bond hydrogenation of 15-deoxy-$\Delta^{12,14}$-prostaglandin J_2 by human prostaglandin reductase 1: Product identification by ^{1}H and ^{13}C NMR spectroscopy and catalytic mechanism** (manuscript in preparation)

4.1. Abstract

15-Deoxy-$\Delta^{12,14}$-prostaglandin J_2 (15d-PGJ_2) is a natural ligand of peroxisome proliferator-activated receptor gamma and a highly reactive electrophilic molecule. Some of the biological effects of 15d-PGJ_2 are mediated through receptor-independent pathways relying on posttranslational protein modification. Inactivation of 15d-PGJ_2 can be achieved by double-bond hydrogenation catalyzed by alkenal/one oxidoreductases, such as prostaglandin reductase 1 (PTGR1). By using ^{1}H and ^{13}C NMR spectroscopy, we have identified two different diastereoisomers, (12*R*)- and (12*S*)-12,13-dihydro-15d-PGJ_2, as the products of human PTGR1 activity, proving the enzymatic hydrogenation of the C12-C13 α,β-double bond. Molecular docking of 15d-PGJ_2 into the crystallographic structure of human PTGR1 predicts three tyrosine residues (Tyr49, Tyr245 and Tyr273) making van der Waals interactions with the substrate and a properly positioned Cβ atom for hydride transfer from the C4 atom of the NADPH nicotinamide. However, Tyr49 is not well oriented while substitution of either Tyr245 or Tyr273 by site-directed mutagenesis yields active enzyme, thus discarding their participation as proton donor residues. Considering these results, we propose a catalytic mechanism where the NADPH hydride first attacks the electrophilic C13 atom, and then protonation of the C12 atom takes place with little stereoselectivity. Since a suitably positioned proton donor residue is not available, a solvent proton could be added from both substrate faces, leading to the formation of the two diastereomeric products. The here described mechanism is also fully

compatible with the hydrogenation of the C13-C14 double bond of 15-keto-PGs by PTGR1.

4.2. Introduction

The isoprostane 15-deoxy-$\Delta^{12,14}$-prostaglandin J_2 (15d-PGJ_2) (Fig. 24), a naturally occurring degradation product of prostaglandin D_2 (PGD_2), is a lipid electrophilic molecule and an important redox signaling mediator with anti-inflammatory and adipocyte differentiating properties. 15d-PGJ_2 is the endogenous ligand of peroxisome proliferator-activated receptor gamma (PPARγ). However, some effects of 15d-PGJ_2 are mediated through receptor-independent pathways. This α,β-unsaturated electrophilic compound preferentially forms 1,4-Michael type adducts with nucleophiles, such as proteins and DNA. The 15d-PGJ_2 molecule contains two electrophilic carbons at positions 9 and 13 which exert distinct contributions to the biological activity of 15d-PGJ_2. While C13 is important for interaction with and activation of PPARγ[66], C9 is the main site for glutathione conjugation and posttranslational protein modification[67]. In fact, several covalent adducts of 15d-PGJ_2 have been reported with specific cysteine residues of proteins such as NF-κB, Keap1, Hras, Tat, etc.[68–72] 15d-PGJ_2 can be inactivated by glutathione conjugation or by enzymatic double-bond hydrogenation[73–75]. Recently, we kinetically characterized and performed site-directed mutagenesis studies on human prostaglandin reductase 1 (PTGR1), also known as leukotriene B_4 dehydrogenase. PTGR1 is a zinc-independent member of the medium-chain dehydrogenase/reductase (MDR) superfamily catalyzing the NADPH-dependent reduction of the α,β-double bond (C13−C14) of 15-*keto*-PGs. It was postulated that the catalytic mechanism of guinea-pig PTGR1 with 15-*keto*-PGE_2 involves an enolate intermediate and the hydride (H_a, pro-*R* atom) transfer of the NADPH

nicotinamide to the *re* face of the substrate Cβ atom[29]. Later, Yu *et al.*[74] studied the 15d-PGJ_2 reduction catalyzed by rat PTGR1 but the authors did not provide the unambiguous identification of the reaction product. In the present work, we analyzed the activity of human PTGR1 with 15d-PGJ_2, identified the reaction products and the reduced double bond by ^{1}H and ^{13}C NMR spectroscopy, and proposed a catalytic mechanism.

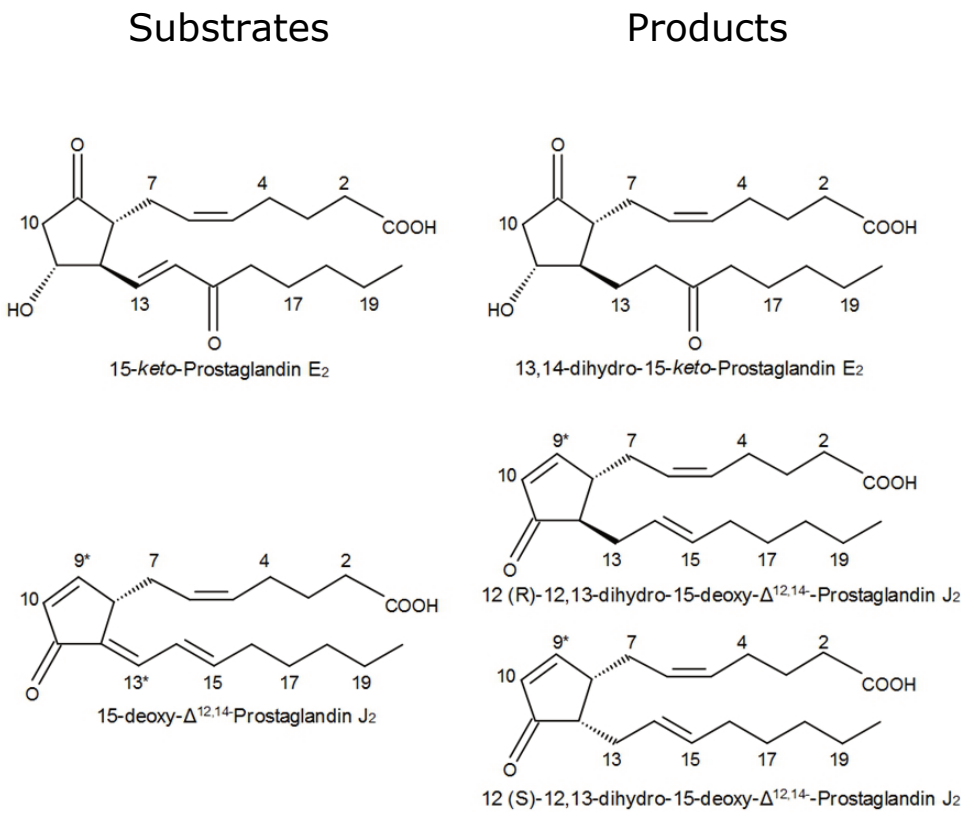

<u>Figure 24:</u> Structures of 15-*keto*-Prostaglandin E_2 and 15-deoxy-$\Delta^{12,14}$-Prostaglandin J_2 used as substrates and their products. Substrates, on the left, and the corresponding products, on the right, after reduction by PTGR1. Asterisks (*) indicate the electrophilic atoms in 15-deoxy-$\Delta^{12,14}$-Prostaglandin J_2.

4.3. Materials and methods

4.3.1 Materials

All compounds were purchased from Cayman Chemical (Ann Arbor, MI). 15d-PGJ_2 was 11-oxo-prosta-5*Z*,9,12*E*,14*E*-tetraen-1-oic acid (CAS number 87893-55-8). LTB_4 was leukotriene B_4 (5*S*,12*R*-dihydroxy-6*Z*,8*E*,10*E*,14*Z*-eicosatetraenoic acid, CAS number 71160-24-2).

4.3.2 Site-directed mutagenesis

The mutants (Arg56Ala, Tyr245Phe and Tyr273Phe) were made using the QuikChange Site-Directed Mutagenesis Kit. We start from pNIC28-Bsa4 construts[60], which allow wild-type PTGR1 protein expression. The primers required for mutagenesis were designed and manufactured with the following sequences: Arg56Ala (5'-GGCAGCCAAA**GC**ATTGAAGGAAGGTGATAC-3' and 5'-CCTTCCTTCAAT**GC**TTTGGCTGCCACTC-3'), for Tyr245Phe (5'-GCCATCTCTACAT**T**TAACAGAACCGGCCCACTTCCC-3' and 5'-GGGCCGGTTCTGTTA**A**ATGTAGAGATGGCTCCAC-3') and for Tyr273Phe (5'-GCTTTTGTCGTCT**T**CCGCTGGCAAGGAGATGCCC-3' and 5'-GGGCATCTCCTTGCCAGCGG**A**AGACGACAAAGC-3'), nucleotide changes are shown bold and underlined.

4.3.3 Protein expression and purification

Human PTGR1 and its mutants (Arg56Ala, Tyr245Phe and Tyr273Phe) were expressed from pNIC28-Bsa4 constructs, which allow protein expression with a $(His)_6$ tag under the control of the T7 RNA polymerase promoter and *lac* operon. For protein expression, *E. coli* BL21(DE3)*pLys* strains transformed with the respective constructs were grown in 25 mL LB medium with 33 µg/mL cloramphenicol and 33 µg/mL kanamycin at 37°C overnight. This culture was used to inoculate 1 L 2x YT medium in the presence of the same antibiotics and was incubated at 37°C until an OD_{600} of 0.6 was reached. Protein expression was then induced by the addition of 0.1 mM IPTG and cells were grown overnight at 22°C. Cells were collected by centrifugation (20 min, 12000 x *g*), resuspended with 50 mL of Bind Buffer (20 mM Tris-HCl, 0.5 M NaCl, 5 mM imidazole, pH 8) per litre of cell culture and stored frozen at −20°C until use. For protein purification, cell lysis was performed by treatment with 1 mg/mL lysozyme, 20 µg/mL DNase and 1 mM of protein inhibitor PMSF (Sigma-Aldrich) followed by 2 cycles of 2-min sonication. The resulting cell homogenate was centrifuged (20 min, 12000 x *g*), cleared through filtration and applied to a 5-mL Hi-Trap™ (GE Healthcare) column using an ÄKTA™ FPLC (GE Healthcare) purification system. The protein was eluted by applying a step-wise gradient of increasing imidazole (5, 60, 100 and 250 mM) concentration. The enzyme eluted at 250 mM imidazole and the corresponding fractions were collected. The imidazole present in the eluted protein fractions was removed through a PD-10 column (*GE Healthcare*). The proteins including the His tag were stored frozen at −80°C in 200-µL aliquots. To follow the purification

process, 1-mL aliquots were collected from each step and analyzed by SDS-polyacrylamide gel electrophoresis.

4.3.4 Kinetic characterization by HPLC-based method

Reaction mixtures were prepared in 100 mM sodium phosphate, pH 7.0, 0.2 mM NADPH, and enzyme, in glass tubes up to 1-mL total volume. Reactions were started by the addition of prostaglandin and were incubated at different times and substrate concentrations, at 37°C, to obtain a conversion of substrate to product from 10 to 30%. Just before ending the reaction, 70 µL LTB_4 (1 ng/µL, in 100 mM sodium phosphate) was added as an internal standard. The reaction was stopped by the addition of 2 mL ice-cold ethyl acetate and prostaglandins were extracted by centrifugation at 1200 rpm for 1.5 min at room temperature. The upper layer (80%) was recovered and evaporated under nitrogen. Three-hundred µL of mobile phase (acetonitrile/0.1% formic acid in water, 35:65, v/v) were added, and an aliquot (200 µL) was analyzed by HPLC (Waters Alliance 2695). The column (Symmetry C18 Cartridge, 100 Å, 5 µm, 3 x 150 mm) was eluted with mobile phase at a flow rate of 1.5 mL/min. The absorbance was monitored at 230 nm (for 15d-PGJ_2), 220 nm (for reaction products) and 270 nm (for LTB_4).

4.3.5 Docking simulations

Docking simulations were performed with the program AutoDock 4.2. The ligand was 15d-PGJ_2 and their coordinates were generated by drawing the molecule using Symyx Draw 3.2. To eliminate any potential bond length and bond angle biases in the structure, the ligands were subjected to a full minimization prior to the docking using the PRODRG server (http://davapc1.bioch.dundee.ac.uk/cgi-bin/prodrg). The crystal structure of the ternary complex of the human enzyme with $NADP^+$ and raloxifene (PDB ID: 2Y05), and that of guinea-pig holoenzyme (PDB ID 1V3V) were used as models. The inhibitor molecule was removed and the protein structure and the cofactor were kept rigid, while all the torsional bonds in the ligand, except for all the conjugated double bonds, were set free. Gasteiger united atom partial charges were assigned and polar hydrogen atoms were added by using the Hydrogen module in AutoDock Tools (ADT). The dimensions of the grid were 70 x 70 x 70 Å, with a spacing of 0.375 Å between the grid points, and centered in the coordinates of the Tyr245 hydroxyl group. The ligand docking was accomplished using 200 Lamarckian genetic algorithms (LGA) from random initial position of the ligand. The docking parameters were left as default. Following docking, all structures generated for the same compound were subjected to cluster analysis with a tolerance of 2.0 Å for an all-atom root mean square deviation (rmsd) from a lower energy structure. Figures were prepared using PyMOL.

4.3.6 NMR analysis of PTGR1 reaction products

Reaction mixtures were prepared as described above. Reaction was started by the addition of 15d-PGJ_2 and was incubated enough time at 37°C to obtain a conversion of substrate to product as large as possible. The reaction was stopped by the addition of 2 mL ice-cold ethyl acetate and prostaglandins were extracted by centrifugation at 1200 rpm for 1.5 min at room temperature. The upper layer (80%) was recovered and evaporated under nitrogen. Dry samples were dissolved in $CDCl_3$ and NMR experiments were recorded on a BRUKER DRX-500 spectrometer equipped with a 3-channel 5-mm cryoprobe incorporating a z-gradient coil. The temperature for all measurements was set to 298 K. Full peak assignment of proton absorptions from 15d-PGJ_2 and from the two diastereomeric products was achieved after running the following experiments and registering and analyzing the corresponding spectra: ^{1}H-NMR, ^{13}C-NMR, DEPT-135, Gradient-enhanced magnitude mode COSY (sequence cosygpqf), Phase sensitive ge-2D HSQC (sequence hsqcetgpsisp2), Magnitude mode ge-2D HMBC (sequence hmbcgplpndqf).

4.4. Results and discussion

4.4.1 NMR analysis of human PTGR1 activity with 15d-PGJ_2

Enzymatic activity with 15d-PGJ_2 was determined by an HPLC-based method where the consumption of the prostaglandin substrate was followed (Fig. 25). A single product peak was observed by monitoring the elution profile at 220 nm. In order to identify the enzymatic products, the reaction mixture was submitted to ^{1}H and ^{13}C NMR mono- and two-dimensional spectroscopy. The chemical shifts corresponding to 15d-PGJ_2 could be unambiguously assigned in the reaction mixture prepared in the absence of enzyme (Fig. 26). Careful analysis of new peaks appearing in the reaction mixture in the presence of enzyme revealed a mixture of two different diastereomeric products, (12*R*)- and (12*S*)-12,13-dihydro-15d-PGJ_2 (Fig. 24), as a result of the C12−C13 double bond hydrogenation (Fig. 27). The two diastereoisomers were produced by the reduction through the two diastereotopic faces of the cyclopentenone ring. Attack to the (12*re*) face created a new chiral center with (12*S)* absolute configuration and with substituents on C8 and C12 in *cis*. On the contrary, attack on the (12*si*) face produced the (12*R)* chiral center and the *trans* relative configuration on C8-C12. Expansion and integration of ^{1}H-NMR spectrum indicates that the two novel H8 protons (δ= 3.08 and 2.73) are in a 1:1.47 ratio, corresponding to a diastereomeric excess of 18.9%. The coupling constants deduced from the expansion of the novel H8 protons indicate that the one at δ= 3.08 has five coupling constants with values 10.5, 6, 5, 3, and 2 Hz, while the other (δ = 2.73) presents two couplings with 7.1 Hz and three

with 2.1 Hz (Fig. 28). These couplings are compatible with the presence of the (12*S*) and (12*R*) isomers, respectively.

This result demonstrates that PTGR1 catalyzed the reduction of the α,β-double bond (C12−C13) with respect to the carbonyl group at C11 and has relevant consequences on the catalytic mechanism, as we will discuss below. More importantly, the relative abundance of the two diastereoisomers is consistent with the small selectivity of the protonation step. The two diastereoisomers were produced by the reduction through the two diastereotopic faces of the cyclopentenone ring. Attack to the (12*re*) face created a new chiral center with (12*S)* absolute configuration and with substituents on C8 and C12 in *cis*; on the contrary, attack on the (12*si*) face produced the (12*R)* chiral center and the *trans* relative configuration on C8-C12. No evidence of C9-C10 double bond hydrogenation was found. This result is consistent with what was observed for rat PTGR1, although in that case mass spectrometry was used and could not discriminate between the two double bond positions or the two product isomers[74].

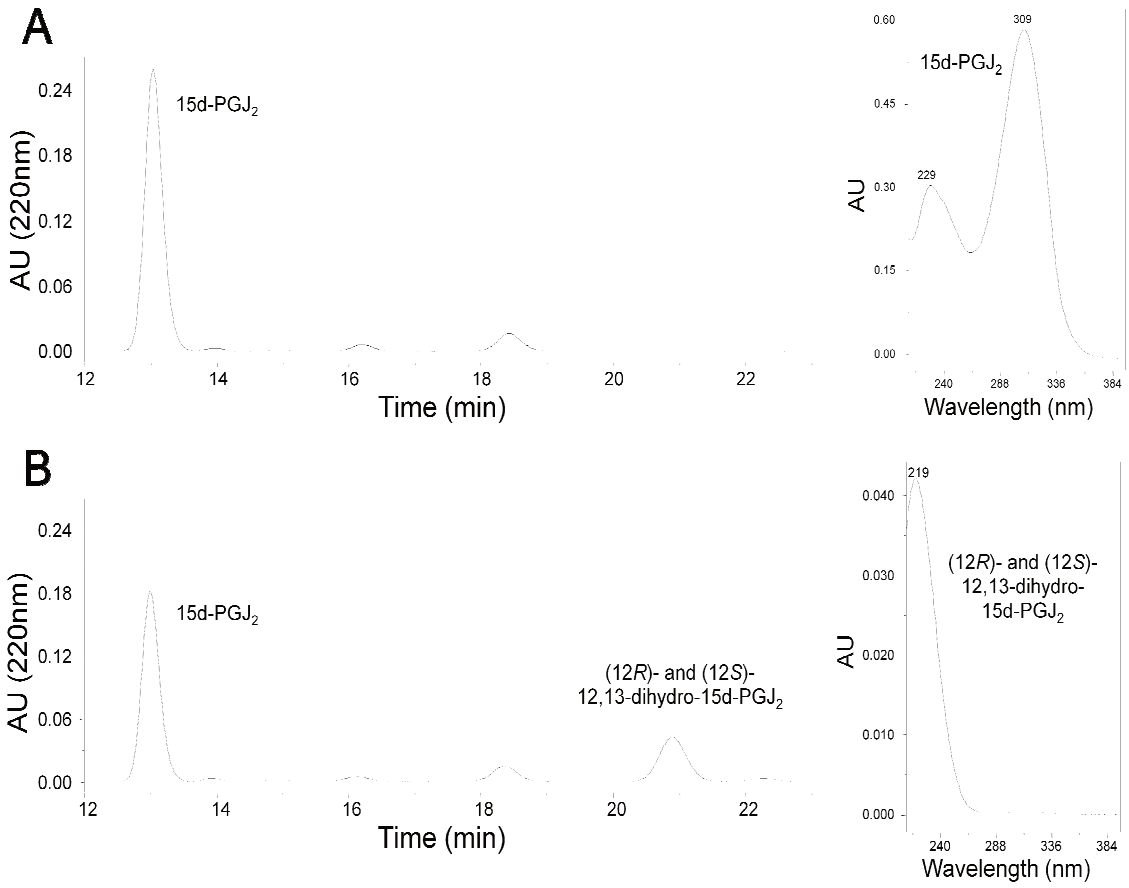

Figure 25: HPLC analysis of the reduction reaction of 15d-PGJ$_2$ by PTGR1. (A) No enzyme was added to the reaction mixture. (B) PTGR1 was added. Left: elution profile of substrate and products. Right: UV–vis absorption spectra of substrate (top) and reaction products (bottom).

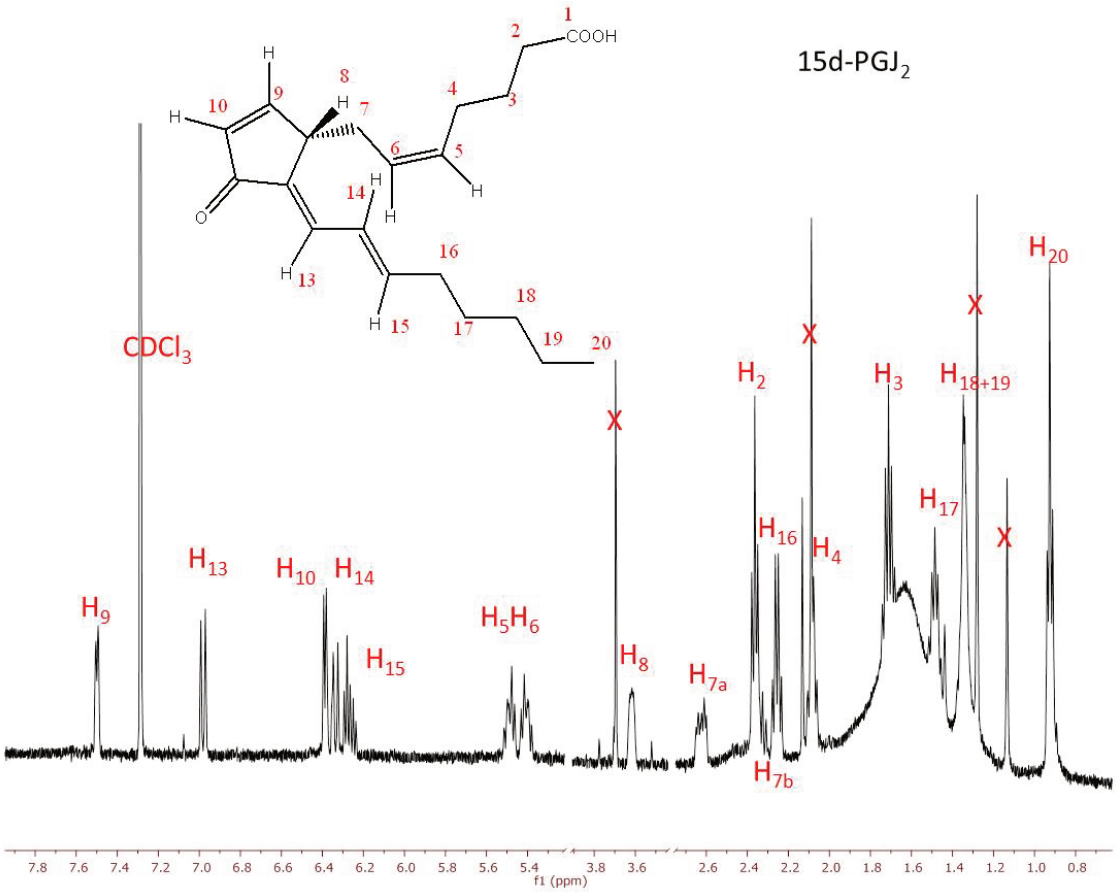

Figure 26: ^{1}H-NMR spectrum of 15d-PGJ_2 in the absence of enzyme, recorded in $CDCl_3$ at 500 MHz and 298 K. Assignment of peaks to 15d-PGJ_2 protons are shown and marked as H_n. Impurities present in the sample are marked as X.

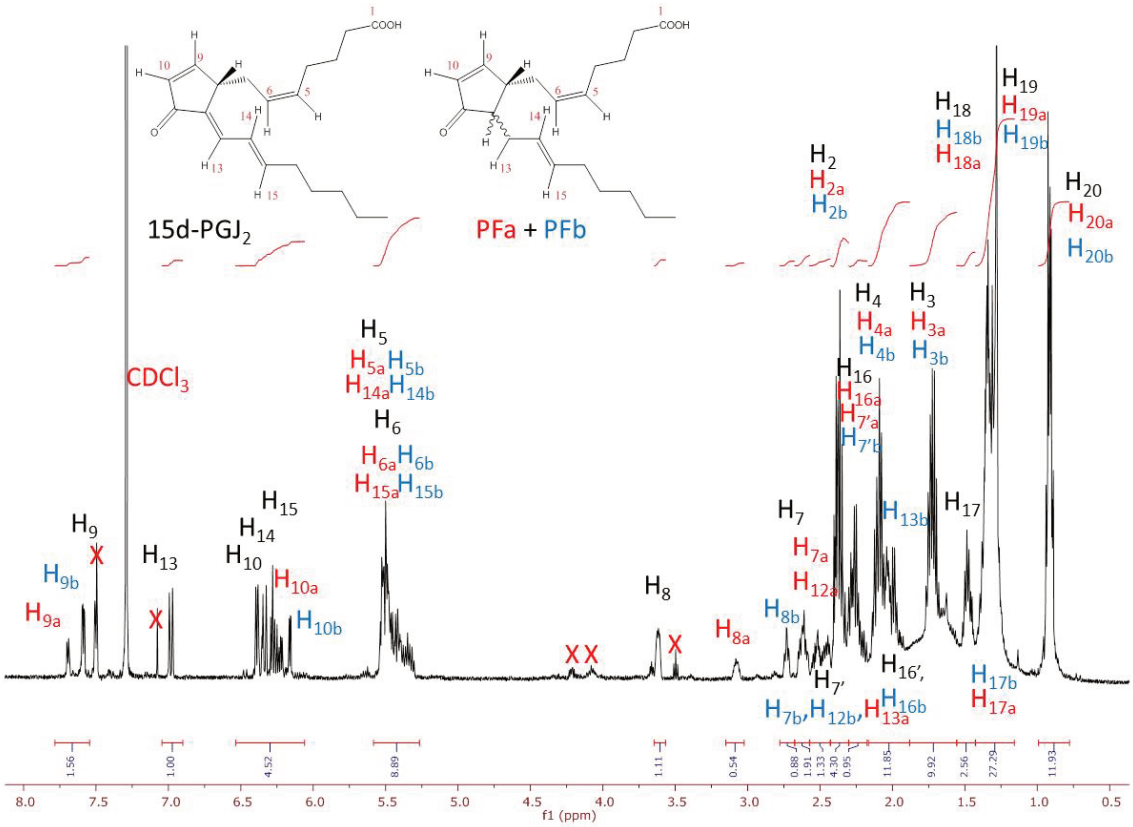

Figure 27: ^{1}H-NMR spectrum of the reduction reaction of 15d-PGJ$_2$ by PTGR1, recorded in $CDCl_3$ at 500 MHz and 298 K. Clearly, two diastereomeric products, apart from the substrate, are observed. Assignment of peaks to the protons from 15d-PGJ$_2$ and from diastereoisomers are shown and marked as H_n (in black), and H_{na} (in red) and H_{nb} (in blue), respectively. $CHCl_3$ side bands as well as some impurities present in the sample are marked as X.

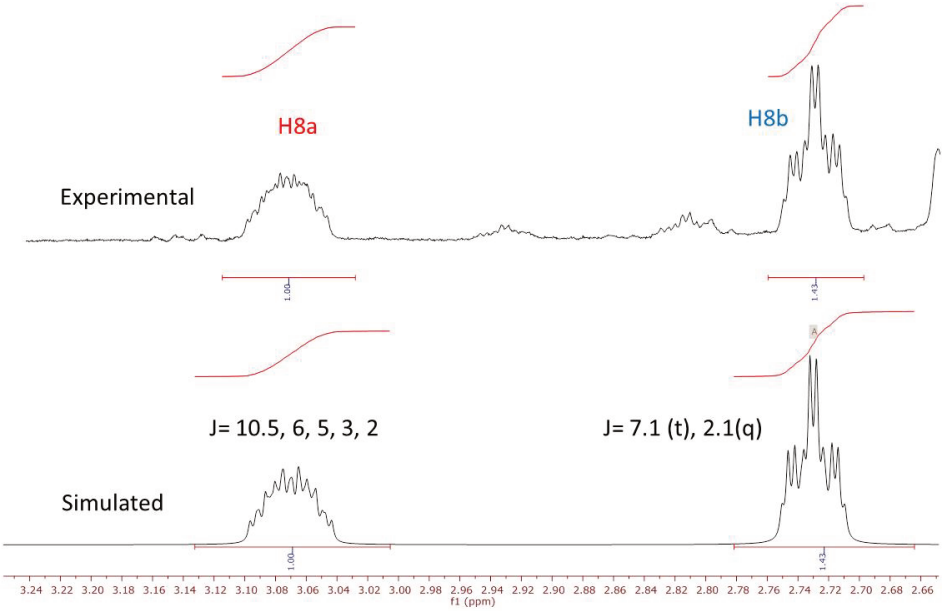

Figure 28: Expansion of a portion of the ^{1}H-NMR spectrum of the products of the enzymatic reduction of 15d-PGJ$_2$ corresponding to the H8 protons of the two diastereomeric products; couplings of 10.5, 6, 5, 3, and 2 Hz, were used for the simulation of the absorption at δ = 3.08, and of 7.1 Hz (t), and 2.1 Hz (q), for the one at δ = 2.73.

4.4.2 Kinetic parameters of PTGR1 with 15d-PGJ_2

PTGR1 catalyzed the NADPH-dependent reduction of 15d-PGJ_2 with a K_m value in the micromolar range (Table 11), similar to that for other 15-*keto*-prostaglandins[19]. The catalytic efficiency of PTGR1 with 15d-PGJ_2 was also comparable to that with other 15-*keto*-PGs. In order to validate the molecular docking predictions, we also examined the effect of various mutations, involving Tyr245, Tyr273 and Arg56, on the kinetic constants (Table 11). The Tyr245 mutant shows a notable decrease in the catalytic efficiency (k_{cat}/K_m) with 15d-PGJ_2, mainly as a consequence of the rise in the K_m value, similar to what had been observed with 15-*keto*-PGE_2[19]. In fact, the Tyr245Phe mutant displays a higher K_m value for 15d-PGJ_2, but the increase (14-fold) is not as large as that previously reported for 15-*keto*-PGE_2 (75-fold,[19]). For this substrate, we proposed the participation of Tyr245 in substrate binding, through the 2'-hydroxyl group of the NADPH ribose, although this Tyr residue was not absolutely required for catalysis[19]. Here, the involvement of Tyr245 in 15d-PGJ_2 binding might be less relevant since the interaction with the 2'-hydroxyl group of the nicotinamide is lost.

No effect on the kinetic constants is observed for the Tyr273Phe mutant, suggesting that this residue is not involved in catalysis or substrate binding. This is supported by the lack of effect of this mutation on the kinetic constants for the model substrate *trans*-2-nonen-3-one (results not shown). The R56A mutation results in a 9-fold decrease in the catalytic efficiency, which parallels our previous observation on this mutant with 15-*keto*-PGE_2[19] and supports the role of Arg56 in establishing an ionic interaction with the α chain carboxyl group of 15d-PGJ_2. This result is

consistent with our molecular docking analysis and confirms the importance of Arg56 for properly positioning of the prostaglandin substrates in the active site. By tethering the carboxyl end of the α chain, the ω chain will be facing the nicotinamide ring to facilitate the hydride transfer on C13.

Table 11. Kinetic parameters of wild-type and mutant PTGR1 with 15-deoxy-$\Delta^{12,14}$-prostaglandin J_2

Parameter	**Wild Type**	**Y245F**	**Y273F**	**R56A**
K_m (μM)	1.8 ± 0.6	25.7 ± 9.6	2.8 ± 0.7	9.9 ± 3
k_{cat} (min^{-1})	2.75 ± 0.32	1.9 ± 0.3	3.8 ± 0.3	1.7 ± 0.2
k_{cat}/K_m ($mM^{-1}\cdot min^{-1}$)	1500 ± 500	76 ± 31	1350 ± 180	170 ± 55

Activities were determined in 0.1 M sodium phosphate, pH 7.0, with 0.2 mM NADPH, at 37°C.

4.4.3 Molecular docking of 15d-PGJ_2 into the PTGR1 active site

The crystal structure of human PTGR1 (PDB ID 2Y05) was used as a template to dock the 15d-PGJ_2 molecule into the active site of human PTGR1 (Fig. 30). The substrate could be fitted into the substrate-binding site with a favorable binding energy ($\Delta G = -7.2$ kcal/mol). The atomic distance between the C4 of nicotinamide NADPH and the Cβ (C13) of 15d-PGJ_2 was 4 Å, very similar to that measured in the PTGR1 structure with the C13 of 15-*keto*-PGE_2 (3.8 Å)[29]. In contrast to the complex with 15-*keto*-PGE_2, the interaction of the 2'-hydroxyl group of the nicotinamide ribose with the substrate was lost due to the absence of the carbonyl group at C15 in 15d-PGJ_2. A new interaction could be predicted, involving the Tyr273 hydroxyl group and the carbonyl oxygen of C11 (Fig. 29). However, as shown below, site-directed mutagenesis results do not give support to this observation. Finally, the carboxyl group in the prostaglandin α chain ionically interacts with Arg56 (Fig. 29), as previously suggested for 15-*keto*-PGs[19], and here supported by the kinetic analysis of the Arg56Ala mutant.

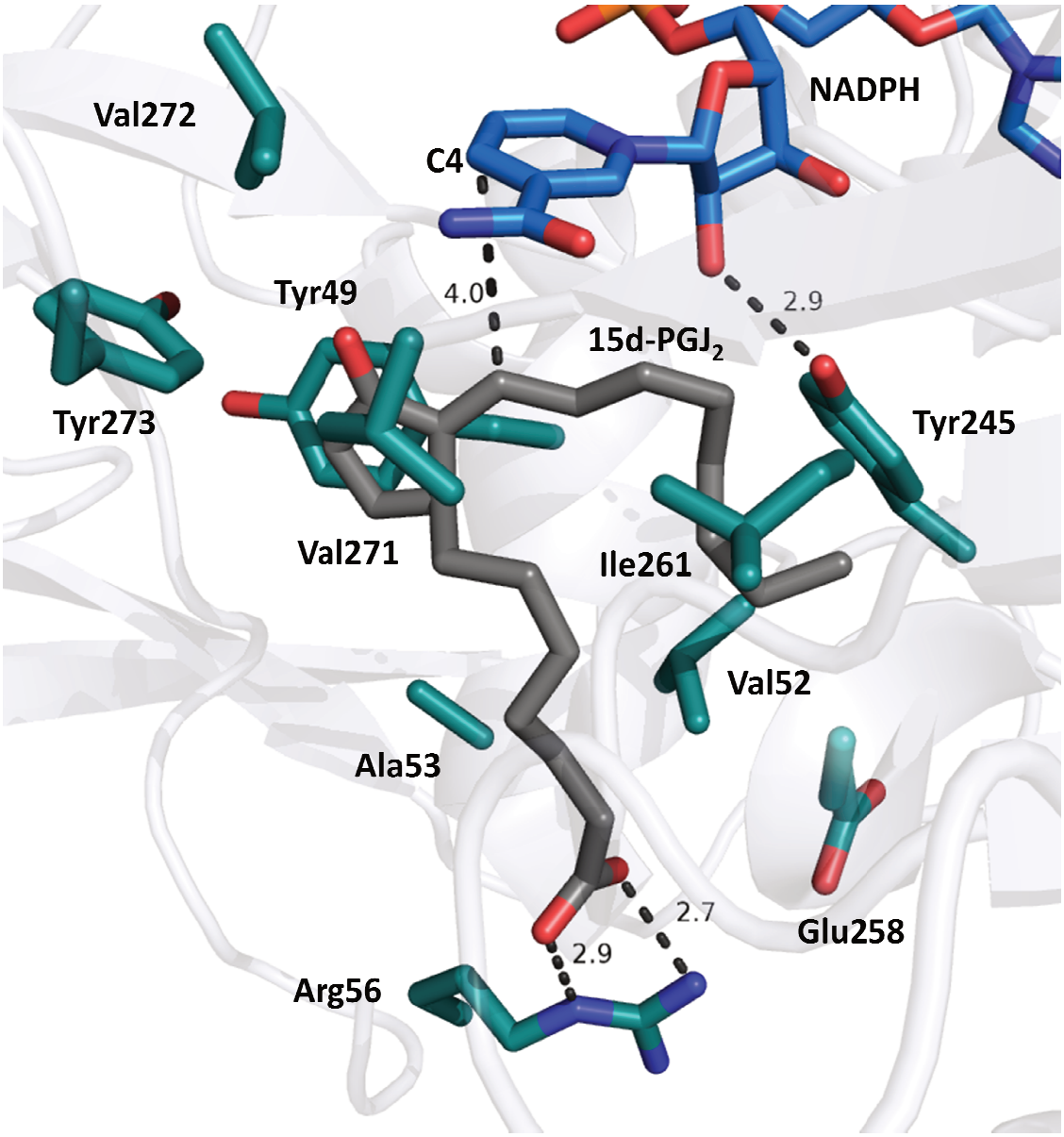

Figure 29: Docking simulation of 15d-PGJ$_2$ bound into the PTGR1 active site. The structure of the human PTGR1 structure (PDB ID 2Y05) is shown. Tyr245 forms a hydrogen bond with the 2′-hydroxyl group of the nicotinamide ribose (2.9 Å). The distance between the C4 atom of the nicotinamide and Cβ of the substrate is shown (4.0 Å). A predicted ionic interaction between Arg56 and the substrate carboxyl group is depicted. Residues involved in van der Waals interactions are shown: Tyr49, Val52, Ala53, Tyr245, Glu258, Ile261, Val271, Val272 and Tyr273.

4.4.4 Proposed catalytic mechanism

C9 and C13 (both are Cβ atoms) are the two most electrophilic positions in 15d-PGJ_2, but only C13 would be located at the right distance for hydride transfer from the C4 of the NADPH nicotinamide (Fig. 29). This would explain why the 9,10 double bond is not reduced or why the 1,4-addition is preferred over the 1,6-addition reaction (14,15 double bond reduction). In fact, based on the NMR analysis of the reaction products, only the C12-C13 double bond is enzymatically reduced, resulting in the synthesis of two epimers. Thus, we propose the following catalytic mechanism for the hydrogenation of the C12-C13 double bond of 15d-PGJ_2 (Fig. 30B and 31).

Any α,β-unsaturated ketone presents a resonant form where a partial positive charge is created on the Cβ atom. As in the cases of guinea-pig PTGR1 (Fig. 30A), Arabidopsis AOR, human PTGR2 and ζ-crystallin, where a conjugated enolate was proposed as the reaction intermediate with the participation of a Tyr residue[20,29,35,76], in our substrate this positive charge density would be created at C13. The proposed mechanism would be based on orientation and proximity effects in addition to the higher substrate reactivity of 15d-PGJ_2. The reaction could then proceed stepwise or by a concerted mechanism through the nucleophilic attack by the NADPH hydride on the electrophilic C13 atom. Enzymes of the MDR superfamily are all pro-(4*R*) specific and the hydride transfer takes place on the *re* or *si* face of the substrate. In the action of PTGR1 on 15d-PGJ_2, the hydride attack occurs on the *si* face. As a second step, a proton from the solvent or a proton donor residue, such as His, Ser or Tyr[77], could be transferred to the O11 atom of

the enolate anion. In the available 3D structures of PTGR1, the substrate ω chain is solvent accessible. A properly positioned proton donor residue is not available and a solvent proton or the keto-enol tautomerism would favor the addition at C12 from both substrate faces, therefore explaining the formation of the two diastereomeric products. Product racemization is another possibility but it is unlikely to occur once the reaction mixture is extracted in non-aqueous solvents. The postulated mechanism is consistent with the observation of the protonation step in MDR alkenal/one oxidoreductases and enoyl reductases, being less stereospecific than the hydride transfer step[35,36,78,79]. The proposed mechanism is also fully compatible with the hydrogenation of the C13-C14 double bond of 15-*keto*-PGs by PTGR1[19] but there the lower reactivity of the C13 atom has to be assisted by the stabilization of the enolate intermediate through a hydrogen bond interaction with NADPH and Tyr245. Although the position of the carbonyl group in the active site is shifted by four C atoms (C11 in 15-*keto*-PGs and C15 in 15d-PGJ_2), the Cβ atoms (C13 in both 15-*keto*-PGs and 15d-PGJ_2) are fully superimposable and optimally positioned for hydride transfer (Fig. 29). In the case of 15-*keto*-PGs, though, only a single chemical entity would be formed since protonation of C14 does not yield an asymmetric carbon. Recently, Rosenthal *et al.* (2013, 2015)[63] reported that, for the reduction of the α,β-double bond by MDR crotonyl-CoA carboxylase/reductase, the catalytic mechanism would proceed through a covalent adduct intermediate with NADPH. In that case, a short distance (3.8 Å) between the C2 atom of NADPH and the substrate Cα, and a π-π orbital interaction were required. For PTGR1, the distance between the C2 atom of NADPH and the substrate Cα is 6.1 Å and the relative position of

the two double bonds (C2-C3 of nicotinamide and C12-C13 of 15d-PGJ_2) is not optimal for the ene reaction to take place. Finally, we did not observe any spectrophotometric evidence of such a covalent adduct intermediate.

To our knowledge, this is the first report showing the production of two different molecular entities, (12*R*)- and (12*S*)-12,13-dihydro-15d-PGJ_2, arising from the metabolic inactivation of 15d-PGJ_2. This finding may be relevant as to physiological implications of prostaglandin metabolism and signaling. Future work will have to include their detection at physiological level and investigate whether they might have distinct biological activities.

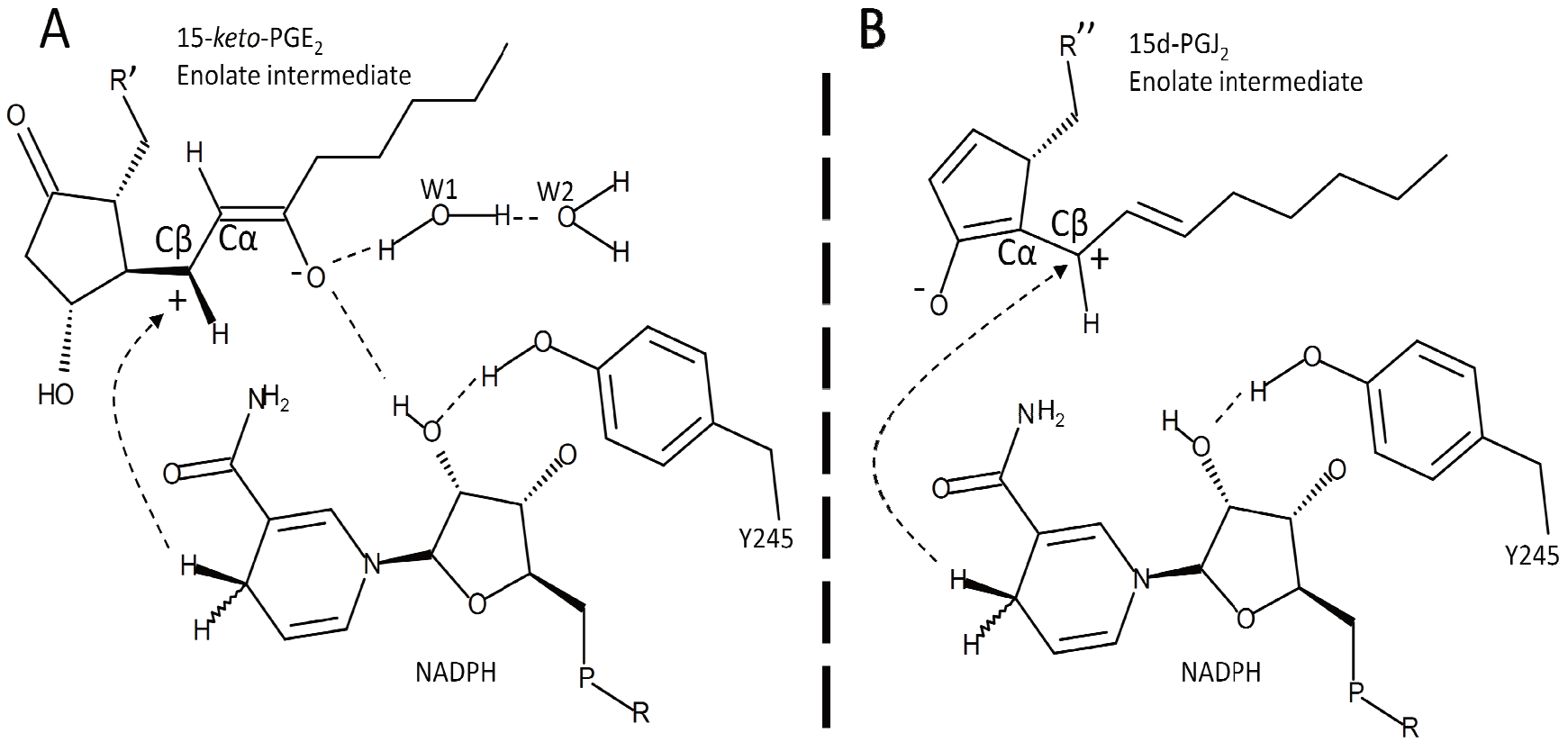

Figure 30: Schematic drawing of the reaction yielding to the enolate anion intermediate in the PTGR1 reductase catalytic mechanism on two different substrates (A) 15-*keto*-PGE_2 (Hori et al., 2004) and (B) 15d-PGJ_2.

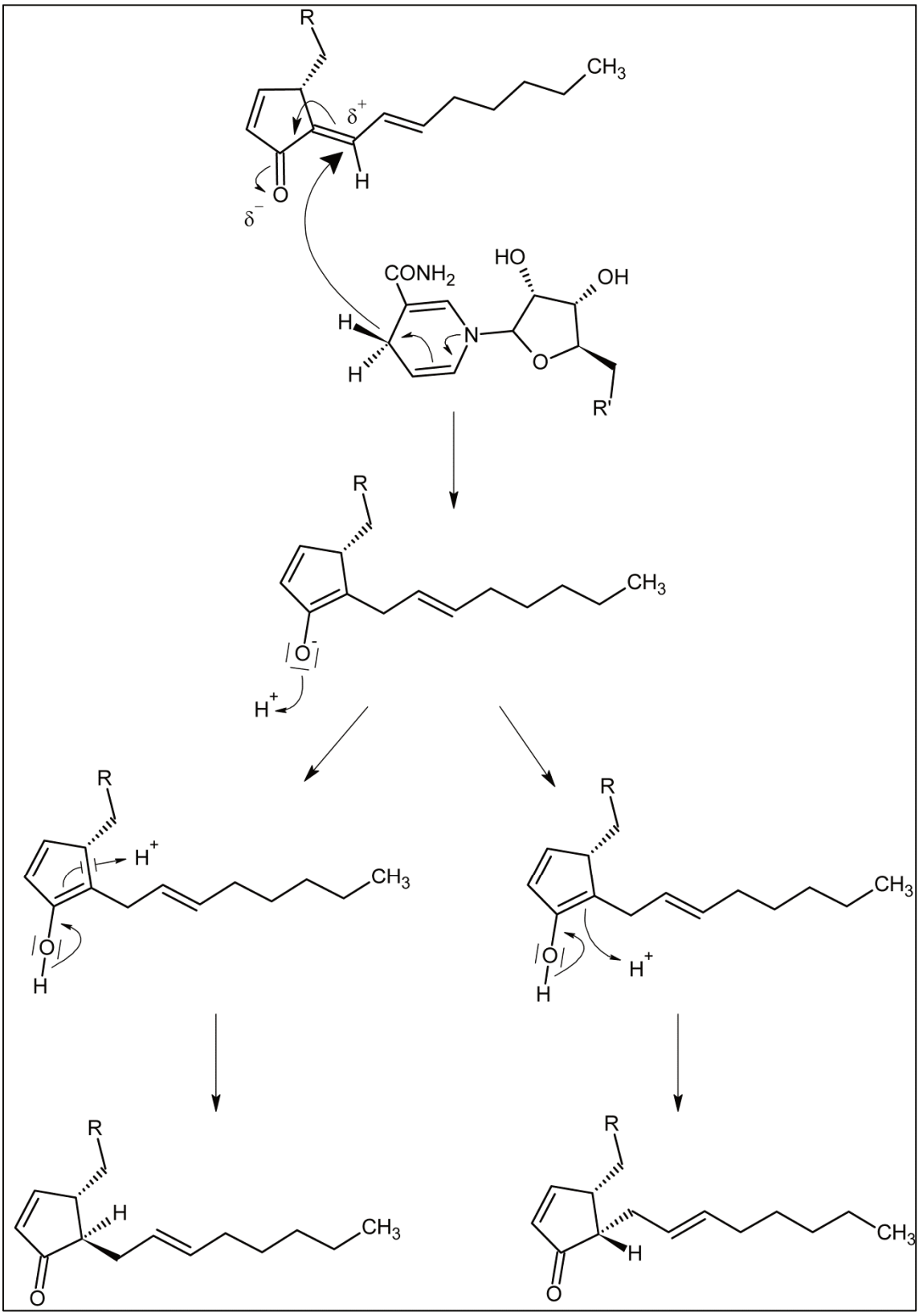

Figure 31:.Proposed catalytic mechanism for the reduction of 15d-PGJ_2 by PTGR1, using NADPH as a cofactor, leading to the two diastereomeric products, (12*R*)- and (12*S*)-12,13-dihydro-15d-PGJ_2.

5. GENERAL DISCUSSION

5. GENERAL DISCUSSION

The current post-genomic era faces enormous challenges in deciphering the role of genes for which a biological function has not yet been fully elucidated to date. The number of human genes without known function could be as high as 24%[80]. Nowadays, to reverse this fact constitutes one of the main objectives of the so called field of functional genomics. Knowledge about existing gene families and the ever-increasing number of 3D structures (for a total of 120,000 released atomic coordinate entries, 32,000 human, approx. 1400 unique folds, 2500 unique superfamilies, in the PDB up to June 2016) provides the opportunity to extrapolate information from homologous proteins, giving clues about their likely biological function. Additional evidence comes from the field human molecular genetics, as genetic linkage analysis, genome-wide association studies and allelic variants provide some knowledge about disease-associated genes, physiological and pathological function, and the role of specific amino acid residues.

Many of the oxidoreductases of phase I-drug metabolism typically fulfill dual roles, firstly in detoxication and defense against oxidative stress, and secondly in the metabolism of signaling molecules. Some of them have acquired through evolution additional catalytic capabilities (dual or multifunctional activities) or even non-enzymatic functions and thus they have been described as being moonlighting proteins or the products of gene sharing. In addition, interest for these enzymes stems from the fact that they are induced or repressed in response to different stimuli and disease states, such as cancer.

The members of the MDR superfamily are no exception. Among these, the Zn-lacking, NADP(H)-dependent MDRs, have long remained much less characterized than MDRs containing Zn and for many of them their enzymatic activity and endogenous substrate are still unknown. We previously characterized the activity of human ζ-crystallin and PIG3. In addition to performing the reduction of quinones, ζ-crystallin catalyzed the double-bond α,β-hydrogenation of medium-chain 2-alkenals and 3-alkenones, while PIG3 performed the hydrogenation of the N=N double bond of the azodicarbonyl diamide and the N=C double bond of 2,6-dichloroindophenol. Thus, the α,β-double bond hydrogenation of carbonyl compounds is not unique to AORs and ETRs but shared by other members of the Zn-independent MDRs. In fact, we have now confirmed that PTGR1 does not reduce the carbonyl group. Instead the conjugated double bond is dehydrogenated. Structural data and site-directed mutagenesis studies support the participation of strictly conserved Tyr residues in the catalytic mechanism, although with distinct roles and requirements (Table 12). In some cases, these Tyr residues are located in homologous positions in the primary sequence (i.e. Tyr245 in PTGR1, Tyr259 in PTGR2, and Tyr260 in Arabidopsis AOR), in other cases, they are not but they are in the appropriate position for catalysis. A special case is that of ζ-crystallin, with two different Tyr residues (Tyr53 and Tyr59) located near the active site with different roles depending on the substrate[76].

Table 12. Role of strictly conserved Tyr residues in Zn-independent MDRs

Enzyme	Species	Tyr	Mutation	Effect	Role	Reference
PTGR1	Guinea pig	245	–	–	Proton donor to NADPH 2′-hydroxyl	[29]
PTGR1	Rat	245	Y245F	No reduction *(R)*- or *(S)*-perillaldehyde. Smaller effect with 1-octen-3-one and *trans*-methyl 4-oxo-2-pentenoate.	Hydrogen bond with $NADP^+$ 2′-hydroxyl, which in turn hydrogen bonds substrate carbonyl	[36]
		262	Y262F	Increase activity with *(S)*-perillaldehyde. 90% less activity with 1-octen-3-one.		
PTGR1	Human	245	Y245F Y245A	Increase in Km value for substrates	Hydrogen bond with $NADP^+$ 2′-hydroxyl, which in turn hydrogen bonds substrate carbonyl. Substrate binding	[19]
		273	Y273F	No effect	No role in catalysis	J. Mesa, unpublished results
PTGR2	Human	259	Y259F	Catalytic efficiency reduced by 43-70%	Hydrogen bond with $NADP^+$ 2′-hydroxyl is important for catalysis	[20]
		64	Y64F		-	
AOR	Arabidopsis	260	–	–	General acid/base for hydride transfer	[35]
MECR /ETR1	Human	94	Y94F	Increase in Km	Important for catalysis	[15]
PIG3	Human	51	Y51F Y51A	Significant increase in kcat/Km	Not the catalytic acid/ base	[81]
ζ -crystallin	Human	59	Y59F Y59A	No effect	Not essential for catalysis	

Interestingly, like MDRs, some members from other oxidoreductase superfamilies also show a dual hydrogenating capability *versus* a carbonyl group or a double bond. In the case of human aldo-keto reductase AKR1D1, a Tyr residue (Tyr58) is the proton donor in both reaction types. A shift in the position of the steroid substrate changes the recipient group for hydride transfer, so that either the steroid double bond or ketone group is positioned for reduction. In short-chain dehydrogenase/reductases, a similar change is achieved by repositioning of the catalytic Tyr^{82}. This magnificently illustrates the importance of orientation and positioning of the chemical groups involved in catalysis and the plasticity of active sites to adapt to various chemical reactions.

A Tyr residue is clearly the proton donor for the hydrogenation of α,β-double bonds in AKRs and SDRs. This is not the case in PTGR1, where Tyr is hydrogen bonding to the 2'-hydroxyl of NADPH ribose. For some substrates, such as 15-*keto*-PGs, the NADPH hydroxyl interacts in its turn with the substrate carbonyl group. This could stabilize the enolate intermediate and facilitate catalysis but this Tyr would not act as a proton donor in acid/base catalysis. For other substrates, such as 15d-PGJ_2, the carbonyl group is out of the range for this interaction and thus would not be able to contribute to the enolate intermediate. The study of the latter hydrogenation, taking place from both faces of C12, and its two diastereomeric products, (12*R*)- and (12*S*)-12,13-dihydro-15d-PGJ_2, has provided invaluable information about the likely reaction mechanism. At least in this case, the solvent seems to be the proton donor.

An important contribution of the present work is the development and validation of a new HPLC-based, end-point analysis method for an accurate measure of 15-*keto*-PGs activity. This was deemed as necessary because previously the 15-*keto* prostaglandin reductase activity had been determined by direct and indirect spectrophotometric methods, which show some limitations when using submicromolar substrate concentrations. Using this method, we have characterized the kinetic parameters of PTGR1 with four different 15-*keto*-PGs, LTB_4 and 15-deoxy-$\Delta^{12,14}$-PGJ_2. In a separate study, we have also checked human PTGR2 and PTGR3 activity with the same substrates and using the same methodology (J. Mesa, unpublished results).

A remarkable new finding of this work, not previously reported, is the role of Arg56 residue of PTGR1 in substrate binding. Previously, the only 3D structure for a ternary complex with a PG substrate was that of guinea-pig PTGR1 with 15-*keto*-PGE_2[29] (PDB ID 1V3V). However, only the ω-side chain of PG was visible in the crystal structure and thus the aliphatic side chain with the terminal carboxylic group could not be solved in this structure. Current molecular docking simulations and site-directed mutagenesis assays have indicated that Arg56 plays an important role in binding the α-chain carboxylic group of 15-*keto*-PGE_2 and 15d-PGJ_2 through an ionic interaction. Interestingly, Arg56 from the human and guinea-pig enzymes is replaced by another basic residue, Lys in other species, such as rat[52] and pig[9]. The Arg56Ala mutation results in a 17-fold decrease in the catalytic efficiency with 15-*keto*-PGE_2 and in a 9-fold decrease in the catalytic efficiency with 15d-PGJ_2. This result is consistent with our molecular docking analysis and confirms the importance of Arg56 for properly positioning the PG substrates

in the active site. The inclusion of *trans*-3-nonen-2-one in the study has added an interesting aspect, as this substrate lacks the carboxylic acid group present in 15-*keto*-PGs, and consistently the Arg56 mutation does not cause any significant effect. The interaction of the carboxylic acid group with a basic residue (Arg or Lys) is also important for recognition between PGH_2 and PGD synthase[83] or between PGE_2 and its receptor subtypes[84]. Arg56 was previously noted to be important for inhibitor binding in the guinea-pig PTGR1 structure in complex with indomethacin (PDB ID 2DM6)[30]. We also predicted that some of the best human PTGR1 inhibitors, niflumic acid and indomethacin would establish ionic interactions with Arg56 through their carboxylic acid group. Therefore, the carboxylic acid stands as a good candidate pharmacophore group in the search of new inhibitors.

Despite the likely physiological role of PTGR1 in PG metabolism, few works have searched for inhibitors of this enzyme. Up to date, only a preliminary screening using some NSAIDs was performed against pig PTGR[54], and the structure of few ternary complexes with pharmacological drugs have been reported[30]. Our work reports the IC_{50} values for several NSAIDs as human PTGR1 inhibitors, showing niflumic acid and indomethacin as the best inhibitors and highlighting the importance of a carboxylic acid group as a pharmacophore. This finding should facilitate the design of more selective inhibitors which could be tested as pharmacological drugs in human therapy (e.g. chemoprevention[50], tumor suppression[46,47] and activation of antitumor drugs[49,52]). This is especially relevant in those cases where PTGR1 upregulation is related to cancer disease. For instance, PTGR1 inhibitors could be used to increase the physiological levels of 15-*keto*-PGE_2, which has been proposed to mediate the anti-proliferative response

described for 15-PGDH[64,65], the enzyme catalyzing the previous step in the same catabolic pathway. The IC_{50} values for indomethacin obtained in the present work (3.2-8.7 μM) are much lower than the value (IC_{50} = 97.9 μM) reported by Hori et al.[30], using guinea-pig PGR1 and 100 μM 15-*keto*-PGE_2 or the value of 180 μM, using human PTGR2 and 200 μM 15-*keto*-PGE_2 [20]. As approved and prescribed COX inhibitors, it is also relevant to provide some comparison regarding inhibitory potency. Thus, for indomethacin, the IC_{50} values of COX-1 and COX-2 are 0.08-0.42 and 0.96-2.75 μM, respectively[85]. For niflumic acid, the IC_{50} values of COX-1 and COX-2 are 16 and 0.1 μM, respectively[86].

In summary, we established a novel method for measuring the enzymatic activity on PGs, investigated the substrate specificity of human PTGR1 with α,β-unsaturated alkenals and alkenones, delineated the role of important active-site residues and explored the inhibitory potency of several NSAIDs. These inhibitors may be of interest for undertaking further studies on the enzyme mechanism and for possible pharmacological applications. In addition, we identified the reaction products of human PTGR1 with 15d-PGJ_2, which allowed us to propose a catalytic mechanism.

6. CONCLUSIONS

6. Conclusions

1. The newly developed HPLC-based method, using end-point product analysis, is highly robust and quantitative, with good reproducibility and precision, showing an extraction efficiency higher than 90%.
2. By using this method, the conversion of 15-*keto*-PGs, 15-deoxy-$\Delta^{12,14}$-PGJ_2 and leukotriene B_4 to their respective reaction products (13,14-dihydro-15-*keto*-PGs, (12*R*)- and (12*S*)-12,13-dihydro-15d-PGJ_2 and 12-*keto*-leukotriene B_4) could be measured and kinetic parameters could be determined.
3. Human PTGR1 is an efficient catalyst in the reduction of α,β-double bonds of medium- and long-chain aliphatic aldehydes and ketones.
4. The best substrates of PTGR1 in terms of catalytic efficiency are 15-*keto*-PGs, especially 15-*keto*-PGE_2.
5. Arg56 is important for PG binding through ionic interaction with the carboxyl group of the substrate side chain.
6. The inhibitory potency of indomethacin and niflumic acid against the PTGR1 activity could be of interest for undertaking further studies on the enzyme mechanism and for possible pharmacological applications.
7. Enzymatic activity of PTGR1 with 15d-PGJ_2 produce two different diastereomeric products, (12*R*)- and (12*S*)-12,13-dihydro-15d-PGJ_2.

8. We propose a catalytic mechanism of PTGR1 in front 15d-PGJ_2 that explains the 12,13 double-bond hydrogenation and the formation of two diastereoisomers.

7. REFERENCES

7. References

1. Hedlund, J., Jörnvall, H. and Persson, B. **Subdivision of the MDR superfamily of medium- chain dehydrogenases/reductases through iterative hidden Markov model refinement** *BMC Bioinformatics* **11,** 534 (2010).
2. Rossmann, M.G., Moras, D., and Olsen, K. W. **Chemical and biological evolution of nucleotide-binding protein** *Nature* **250,** 194–199 (1974).
3. Persson, B., Hedlund, J., and Jörnvall, H. **Medium- and short-chain dehydrogenase/reductase gene and protein families: the MDR superfamily** *Cell. Mol. Life Sci.* **65,** 3879–3894 (2008).
4. Riveros-Rosas, H., Julián-Sánchez, A., Villalobos-Molina, R., Pardo, J. P., and Piña, E. **Diversity, taxonomy and evolution of medium-chain dehydrogenase/reductase superfamily** *Eur. J. Biochem.* **270,** 3309–3334 (2003).
5. Hu, W. H. Hausmann, O.N., Yan, M.S., Walsters, W. M., Wong, P.K., and Bethea, J.R. **Identification and characterization of a novel Nogo-interacting mitochondrial protein (NIMP)** *J. Neurochem.* **81,** 36–45 (2002).
6. Masuda, N., Yasumo, H., Furusawa, T., Tsukamoto, T., Sadano, H., and Osumi, T. **Nuclear receptor binding factor-1 (NRBF-1), a protein interacting with a wide spectrum of nuclear hormone receptors** *Gene* **221,** 225–233 (1998).
7. Yamazoe, M., Shirahige, K., Rashid, M. B., Kaneko, Y., Nakayama, T., Ogasawara, N., and Yoshikawa, H. **A protein which binds preferentially to single-stranded core sequence of autonomously replicating sequence is essential for respiratory function in mitochondria of Saccharomyces cerevisiae** *J. Biol. Chem.* **269,** 15244–15252 (1994).
8. Torkko, J. M., Koivuranta, K.T., Miinalainen, I. J., Yagi, A. I., Shimitz, W., Kastaniotis, A. J., Airenne, T. T., Gurvitz, A., and Hiltunen, K. J. **Candida tropicalis Etr1p and Saccharomyces cerevisiae Ybr026p (Mrf1'p), 2-enoyl thioester reductases essential for mitochondrial respiratory competence** *Mol. Cell Biol.* **21,** 6243–6253 (2001).
9. Ensor, C. M., Zhang, H., and Tai, H. **Purification, cDNA cloning and expression of 15-oxoprostaglandin 13-reductase from pig lung 108,** 103–108 (1998).
10. Yokomizo, T., Izumi, T., Takahashi, T. and Kobayashis, Y. **Enzymatic Inactivation of Leukotriene B4 by a Novel Enzyme Found in the Porcine Kidney Purification and properties of leukotriene B4 12-hydroxydehydrogenase** *J. Biol. Chem.* **268,** 18128–18135 (1993).
11. Rao, P. V, Krishna, C. M. and Zigler, J. S. **Identification and characterization of the enzymatic activity of zeta-crystallin from guinea pig lens. A novel NADPH:quinone oxidoreductase** *J. Biol. Chem.* **267,** 96–102 (1992).

12. Mano, J., Babiychuk, E., Belles-Boix, E., Hiratake, J., Kimura, A., Inze, D., Kushnir, S., and Asada, K. **A novel NADPH:diamide oxidoreductase activity in Arabidopsis thaliana p1 ζ-crystallin** *Eur. J. Biochem.* **267,** 3661–3671 (2000).

13. Vitturi, D. A., Chen, C. S., Woodcock, S. R., Salvatore, S. R., Bonacci, G., Koenitzer, J. R., Stewart, N. A., Wakabayashi, N., Kensler, T. W., Freeman, B. A. and Shopfer F. J. **Modulation of nitro-fatty acid signaling: prostaglandin reductase-1 is a nitroalkene reductase** *J. Biol. Chem.* **288,** 25626–25637 (2013).

14. Dick, R. A., Kwak, M. K., Sutter, T. R. and Kensler, T. W. **Antioxidative function and substrate specificity of NAD(P)H-dependent alkenal/one oxidoreductase. A new role for leukotriene B4 12-hydroxydehydrogenase/15-oxoprostaglandin 13-reductase** *J. Biol. Chem.* **276,** 40803–40810 (2001).

15. Chen, Z. J., Pudas, R., Sharma, S., Smart, O. S., Juffer, A.H., Hiltunen, J.K., Wierenga, R.K., Haapalainen, A.M. **Structural enzymological studies of 2-enoyl thioester reductase of the human mitochondrial FAS II pathway: new insights into its substrate recognition properties** *J. Mol. Biol.* **379,** 830–844 (2008).

16. Massengo-Tiassé, R. P. and Cronan, J. E. **Diversity in enoyl-acyl carrier protein reductases** *Cell. Mol. Life Sci.* **66,** 1507–1517 (2009).

17. Porté, S., Crosas, E., Yakovtseva, E., Biosca, J. A., Farrés, J., Fernández, M. R. and Parés, X. **MDR quinone oxidoreductases: The human and yeast ζ-crystallins** *Chem. Biol. Interact.* **178,** 288–294 (2009).

18. Parés, X., Mesa, J., Alsina, C., Farrés, J., Porté, S. **Kinetic and structural characterization of recombinant human prostaglandin reductase 1 (PGR1)** Abstract presented at the 17th International Workshop on the Enzymology and Molecular Biology of Carbonyl Metabolism, Pennsylvania (USA) (2014).

19. Mesa, J., Alsina, C., Oppermann, U., Parés, X., Farrés, J. and Porté, S. **Human prostaglandin reductase 1 (PGR1): Substrate specificity, inhibitor analysis and site-directed mutagenesis** *Chem. Biol. Interact.* **234,** 105–113 (2015).

20. Wu, Y.H., Ko, T.P., Guo, R.T., Hu, S.M., Chuang, L.M. and Wang, A.H. **Structural basis for catalytic and inhibitory mechanisms of human prostaglandin reductase PTGR2** *Structure* **16,** 1714–1723 (2008).

21. Yu, Y. H., Chang, Y.C., Su, T.H., Nong, J.Y., Li, C.C. and Chuang, L.M. **Prostaglandin reductase-3 negatively modulates adipogenesis through regulation of PPARγ activity** *J. Lipid Res.* **54,** 2391–2399 (2013).

22. Yokomizo, T., Izumi, T. and Shimizu, T. **Leukotriene B4: metabolism and signal transduction** *Arch. Biochem. Biophys.* **385,** 231–241 (2001).

23. Clish, C. B., Levy, B. D., Chiang, N., Tai, H. H. and Serhan, C. N. **Oxidoreductases in lipoxin A4 metabolic inactivation: a novel role for 15-onoprostaglandin 13-reductase/leukotriene B4 12-hydroxydehydrogenase in inflammation** *J. Biol. Chem.* **275,** 25372–25380 (2000).

24. Westbrook, C. and Jarabak J. **Purification and partial characterization of an NADH-linked delta 13-15-ketoprostaglandin reductase from human placenta** *Biochem. Biophys. Res. Commun.* **66,** 541–546 (1975).

25. Westbrook C. and Jarabak, J. **15-ketoprostaglandin delta 13 reductase from human placenta: purification, kinetics, and inhibitor binding** *Arch Biochem Biophys.* **185,** 429-442 (1978).

26. Lee, S. C. and Levine, L. **Purification and properties of chicken heart prostaglandin delta13-reductase** *Biochem. Biophys. Res. Commun.* **61,** 14–21 (1974).

27. Yamamoto, T., Yokomizo, T., Nakao, A., Izumi, T. and Shimizu, T. **Immunohistochemical localization of guinea-pig leukotriene B4 12-hydroxydehydrogenase/15-ketoprostaglandin 13-reductase** *Eur. J. Biochem.* **268,**. 6105–6113 (2001).

28. Yokomizo, T., Ogawa, Y., Uozumi, N., Kume, K., Izumi, T. and Shimizu, T. **cDNA cloning, expression, and mutagenesis study of leukotriene B4 12-hydroxydehydrogenase** *J. Biol. Chem.* **271,** 2844–2850 (1996).

29. Hori, T., Yokomizo, T., Ago, H., Sugahara, M., Ueno, G., Yamamoto, M., Kumasaka, T., Shimizu, T. and Miyano, M. **Structural basis of leukotriene B4 12-hydroxydehydrogenase/15-Oxo-prostaglandin 13-reductase catalytic mechanism and a possible Src homology 3 domain binding loop** *J. Biol. Chem.* **279,** 22615–22623 (2004).

30. Hori, T., Ishijima, J., Yokomizo, T., Ago, H., Shimizu, T. and Miyano, M. **Crystal structure of anti-configuration of indomethacin and leukotriene B4 12-hydroxydehydrogenase/15-oxo-prostaglandin 13-reductase complex reveals the structural basis of broad spectrum indomethacin efficacy** *J. Biochem.* **140,** 457–466 (2006).

31. Zhang, L., Zhang, F. and Huo, K. **Cloning and characterization of a novel splicing variant of the ZADH1 gene** *Cytogenet Genome Res.* **103,** 79–83 (2003).

32. Chou, W.L., Chuang, L.M., Chou, C.C., Wang, A.H., Lawson, J.A., FitzGerald, G.A. and Chang, Z.F. **Identification of a novel prostaglandin reductase reveals the involvement of prostaglandin E2 catabolism in regulation of peroxisome proliferator-activated receptor gamma activation** *J. Biol. Chem.* **282,** 18162–18172 (2007).

33. Chang, E. Y., Tsai, S. H., Shun, C. T., Hee, S. W., Chang, Y. C., Tsai, Y. C., Tsai, J. S., Chen, H. J., Chou, J. W., Lin, S.Y. and Chuang, L. M. **Prostaglandin reductase 2 modulates ROS-mediated cell death and tumor transformation of gastric cancer cells and is**

associated with higher mortality in gastric cancer patients *Am. J. Pathol.* **181,** 1316–1326 (2012).

34. Chang, E. Y., Chang, Y. C., Shun, C. T., Tien, Y. W., Tsai, S. H., Hee, S. W., Chen, I. J., Chuang, L. M. **Inhibition of Prostaglandin Reductase 2 , a Putative Oncogene Overexpressed in Human Pancreatic Adenocarcinoma , Induces Oxidative Stress-Mediated Cell Death Involving xCT and CTH Gene Expressions through 15-Keto-PGE2** *PLoS One* **11,** (2016).

35. Youn, B., Kim, S.J., Moinuddin, S.G., Lee, C., Bedgar, D.L., Harper, A.R., Davin, L.B., Lewis, N.G. and Kang, C. **Mechanistic and structural studies of apoform, binary, and ternary complexes of the Arabidopsis alkenal double bond reductase At5g16970** *J. Biol. Chem.* **281,** 40076–40088 (2006)

36. Bougioukou, D. J. and Stewart, J. D. **Opposite stereochemical courses for enzyme-mediated alkene reductions of an enantiomeric substrate pair** *J. Am. Chem. Soc.* **130,** 7655–7658 (2008).

37. Porté, S. **Estudis Estructurals i Funcionals de les Quinona Oxidoreductases Humanes PIG3 i ζ-crystallin** Doctoral Thesis. Universitat Autònoma de Barcelona (2009).

38. Dick, R. A. and Kensler, T. W. **The catalytic and kinetic mechanisms of NADPH-dependent alkenal/one oxidoreductase** *J. Biol. Chem.* **279,** 17269–17277 (2004).

39. Cebola, I. and Peinado, M. A. **Epigenetic deregulation of the COX pathway in cancer** *Prog. Lipid Res.* **51,** 301–313 (2012).

40. Tai, H. H. **Prostaglandin catabolic enzymes as tumor suppressors** *Cancer Metastasis Rev.* **30,** 409–417 (2011).

41. Surh, Y. J., Na, H. K., Park, J. M., Lee, H. N., Kim, W., Yoon, I. S. and Kim, D. D. **15-Deoxy-$\Delta^{12,14}$-prostaglandin J_2, an electrophilic lipid mediator of anti-inflammatory and pro-resolving signaling** *Biochem. Pharmacol.* **82,** 1335–1351 (2011).

42. Sánchez-Rodríguez, R., Torres-Mena, J. E., De-la-Luz-Cruz, M., Bernal-Ramos, G. A., Villa-Treviño, S., Chagoya-Hazas, V., Landero-López, L., García-Román, R., Rouimi, P., Del-Pozo-Yauner, L., Meléndez-Zajgla, J. and Pérez-Carreón, J. I. **Increased expression of prostaglandin reductase 1 in hepatocellular carcinomas from clinical cases and experimental tumors in rats**. *Int. J. Biochem. Cell Biol.* **53,** 186–194 (2014).

43. Tapak, L., Saidijam, M., Sadeghifar, M., Poorolajal, J. and Mahjub, H. **Competing risks data analysis with high-dimensional covariates: an application in bladder cancer** *Genomics Proteomics Bioinformatics* **13,** 169–176 (2015).

44. Xue, L., Zhu, Z., Wang, Z., Li, H,, Zhang, P., Wang, Z., Chen, Q., Chen, H and Chong, T. **Knockdown of prostaglandin reductase 1 (PTGR1) suppresses prostate cancer cell proliferation by inducing cell cycle arrest and apoptosis** *Biosci. Trends* **10,** 133–139 (2016).

45. Yang, S., Luo, F., Wang, J., Mao, X., Chen, Z., Wang, Z. and Guo, F. **Effect of prostaglandin reductase 1 (PTGR1) on gastric carcinoma using lentivirus-mediated system** *Int. J. Clin. Exp. Pathol.* **8,** 14493–14499 (2015).

46. Zhao, Y., Weng, C. C., Tong, M., Wei, J. and Tai, H. H. **Restoration of leukotriene B4-12-hydroxydehydrogenase/15- oxo-prostaglandin 13-reductase (LTBDH/PGR) expression inhibits lung cancer growth in vitro and in vivo** *Lung Cancer* **68,** 161–169 (2010).

47. Wei, L., Liu, J., Le, X. C., Han, Y., Tong, Y., Lau, A.S. and Rong, J. **Pharmacological induction of leukotriene B4-12-hydroxydehydrogenase suppresses the oncogenic transformation of human hepatoma HepG2 cells** *Int. J. Oncol.* **39,** 735–745 (2011).

48. Cheng, Y., Zhao, J., Tse, H. F., Le, X. C. and Rong, J. **Plant Natural Products Calycosin and Gallic Acid Synergistically Attenuate Neutrophil Infiltration and Subsequent Injury in Isoproterenol-Induced Myocardial Infarction : A Possible Role for Leukotriene B4 12-Hydroxydehydrogenase ?** *Oxid. Med. Cell. Longev.* **2015,** (2015).

49. Yu, X., Erzinger, M. M., Pietsch, K. E., Cervoni-Curet, F. N., Whang, J., Niederhuber, J. and Sturla, S. J. **Up-regulation of human prostaglandin reductase 1 improves the efficacy of hydroxymethylacylfulvene, an antitumor chemotherapeutic agent**. *J. Pharmacol. Exp. Ther.* **343,** 426–433 (2012).

50. Primiano, T., Li, Y., Kensler, T. W., Trush, M. A. and Sutter, T. R. **Identification of dithiolethione-inducible gene-1 as a leukotriene B4 12-hydroxydehydrogenase: implications for chemoprevention** *Carcinogenesis* **19,** 999–1005 (1998).

51. Erzinger, M. M., Bovet, C., Uzozie, A. and Sturla, SJ. **Induction of complementary function reductase enzymes in colon cancer cells by dithiole-3-thione versus sodium selenite** *J. Biochem. Mol. Toxicol.* **29,** 10-20 (2015).

52. Itoh, K., Yamamoto, K., Adachi, M., Kosaka, T. and Tanaka, Y. **Leukotriene B4 12-hydroxydehydrogenase/15-ketoprostaglandin Delta 13-reductase (LTB4 12-HD/PGR) responsible for the reduction of a double-bond of the alpha,beta-unsaturated ketone of an aryl propionic acid non-steroidal anti-inflammatory agent CS-670** *Xenobiotica* **38,** 249–263 (2008).

53. Dick, R. A., Yu, X. and Kensler, T. W. **NADPH alkenal/one oxidoreductase activity determines sensitivity of cancer cells to the chemotherapeutic alkylating agent irofulven** *Clin. Cancer Res.* **10,** 1492–1499 (2004)

54. Clish, C. B., Sun, Y. P. and Serhan, C. N. **Identification of dual cyclooxygenase-eicosanoid oxidoreductase inhibitors: NSAIDs that inhibit PG-LX reductase/LTB(4) dehydrogenase** *Biochem. Biophys. Res. Commun.* **288,** 868–874 (2001).

55. Maier, T. Jenni, S., and Ban, N. **Architecture of mammalian fatty acid synthase at 4.5 A resolution** *Science* **331,** 1258–1262 (2006)

56. Airenne, T. T., Torkko, J. M., Van den plas, S., Sormunen. R. T., Kastaniotis, A. J., Wierenga, R.K. and Hiltunen, J. K. **Structure-function analysis of enoyl thioester reductase involved in mitochondrial maintenance** *J. Mol. Biol.* **327,** 47–59 (2003).

57. Zhang, Y. M., Lu, Y. J. and Rock., C. O. **The reductase steps of the type II fatty acid synthase as antimicrobial targets** *Lipids.* **39,** 1055–1060 (2004).

58. Rosenthal, R. G., Vögeli, B., Quade, N., Capitani, G., Kiefer, P., Vorholt, J..A., Ebert, M.O. and Erb, T.J. **The use of ene adducts to study and engineer enoyl-thioester reductases** *Nat. Chem. Biol.* **11,** 398–400 (2015).

59. Khare, D., Hale, W. A., Tripathi, A., Gu, L., Sherman, D.H., Gerwick, W.H., Håkansson, K. and Smith, J.L. **Structural Basis for Cyclopropanation by a Unique Article Structural Basis for Cyclopropanation by a Unique Enoyl-Acyl Carrier Protein Reductase** *Structure* **23,** 2213–2223 (2015).

60. Savitsky, P., Bray, J., Cooper, C. D., Marsden, B. D., Mahajan, P., Burgess-Brown, N. A. and Gileadi, O. **High-throughput production of human proteins for crystallization: the SGC experience** *J. Struct. Biol.* **172,** 3–13 (2010).

61. Picollo, A., Liantonio, A., Babini, E., Camerino, D. C. and Pusch, M. **Mechanism of interaction of niflumic acid with heterologously expressed kidney CLC-K chloride channels** *J. Membr. Biol.* **216,** 73–82 (2007).

62. Hansen, H. S. **Purification and assay of 15-ketoprostaglandin delta 13-reductase from bovine lung** *Methods Enzymol.* **86,** 156-163. (1982)

63. Rosenthal, R. G., Ebert, M. O., Kiefer, P., Peter, D. M., Vorholt, J. A. and Erb, T. J. **Direct evidence for a covalent ene adduct intermediate in NAD(P)H-dependent enzymes** *Nat. Chem. Biol.* **10,** 50–55 (2014).

64. Lu, D., Han, C. and Wu, T. **15-PGDH inhibits hepatocellular carcinoma growth through 15-keto-PGE2/PPARγ-mediated activation of p21WAF1/Cip1** *Oncogene* **33,** 1–12 (2014).

65. Lu, D., Han, C. & Wu, T. **15-hydroxyprostaglandin dehydrogenase-derived 15-keto-Prostaglandin E2 inhibits cholangiocarcinoma cell growth through interaction with peroxisome proliferator-activated receptor-gamma, SMAD2/3 and TAP63 proteins** *J Biol Chem* **288,** 19484-19502 (2013).

66. Waku, T., Shiraki, T., Oyama, T. and Morikawa, K. **Atomic structure of mutant PPARγ LBD complexed with 15d-PGJ2: Novel modulation mechanism of PPARγ/RXRα function by covalently bound ligands** *FEBS Lett.* **583,** 320–324 (2009).

67. Martínez, A. E., Sánchez-Gómez, F. J., Díez-Dacal, B., Oeste, C. L. and Pérez-Sala, D. **15-Deoxy-Δ(12,14)-prostaglandin J2 exerts**

pro- and anti-inflammatory effects in mesangial cells in a concentration-dependent manner *Inflamm. Allergy Drug Targets* **11,** 58–65 (2012).

68. Kalantari, P., Narayan, V., Henderson, A. J. and Prabhu, K. S. **15-Deoxy- 12,14-prostaglandin J2 inhibits HIV-1 transactivating protein, Tat, through covalent modification** *FASEB J.* **23,** 2366–2373 (2009).

69. Kansanen, E., Kivelä, A. M. and Levonen, A.-L. **Regulation of Nrf2-dependent gene expression by 15-deoxy-Delta12,14-prostaglandin J2** *Free Radic. Biol. Med.* **47,** 1310–1317 (2009).

70. Pérez-Sala, D., Cernuda-Morollón, E. and Cañada, F. J. **Molecular basis for the direct inhibition of AP-1 DNA binding by 15-deoxy-Delta 12,14-prostaglandin J2** *J. Biol. Chem.* **278,** 51251–51260 (2003).

71. Renedo, M., Gayarre, J., García-Domínguez, C. A., Pérez-Rodríguez, A., Prieto, A., Cañada, F. J., Rojas, J. M. and Pérez-Sala D. **Modification and activation of Ras proteins by electrophilic prostanoids with different structure are site-selective** *Biochemistry* **46,** 6607–6616 (2007).

72. Wall, S. B., Oh, J. Y., Mitchell, L., Laube, A. H., Campbell, S. L., Renfrow, M. B. and Landar, A. **Rac1 modification by an electrophilic 15-deoxy Δ(12,14)-prostaglandin J2 analog** *Redox Biol.* **4,** 346–354 (2015).

73. Sanchez-Gomez, F. J., Cernuda-Morollón, E., Stamatakis, K. and Pérez-Sala, D. **Protein thiol modification by 15-deoxy-Delta 12,14-prostaglandin J2 addition in mesangial cells: role in the inhibition of pro-inflammatory genes** *Mol. Pharmacol.* **66,** 1349–1358 (2004).

74. Yu, X., Egner, P. A., Wakabayashi, J., Wakabayashi, N., Yamamoto, M. and Kensler, T.W. **Nrf2-mediated Induction of cytoprotective enzymes by 15-deoxy-Delta 12,14-Prostaglandin J2 is attenuated by alkenal/one oxidoreductase** *J. Biol. Chem.* **281,** 26245–26252 (2006).

75. Koyani, C. N., Windischhofer, W., Rossmann, C., Jin, G., Kickmaier, S., Heinzel, F. R., Groschner, K., Alavian-Ghavanini, A., Sattler, W. and Malle, E. **15-deoxy-$\Delta^{12,14}$-PGJ_2 promotes inflammation and apoptosis in cardiomyocytes via the DP2/MAPK/TNFα axis** *Int. J. Cardiol.* **173,** 472–80 (2014).

76. Porté, S., Moeini, A., Reche, I., Shafqat, N., Oppermann, U., Farrés, J. and Parés, X. **Kinetic and structural evidence of the alkenal/one reductase specificity of human ζ-crystallin** *Cell. Mol. Life Sci.* **68,** 1065–1077 (2011).

77. Steinkellner, G., Gruber, C. C., Pavkov-Keller, T., Binter, A., Steiner, K., Winkler, C., Lyskowski, A., Schwamberger, O., Oberer, M., Schwab, H., Faber, K., Macheroux, P. and Gruber, K. **Identification of promiscuous ene-reductase activity by mining structural databases using active site constellations**. *Nat. Commun.* **5,** 1–9 (2014).

78. Erb, T. J., Brecht, V., Fuchs, G., Müller, M. and Alber, B. E. **Carboxylation mechanism and stereochemistry of crotonyl-CoA carboxylase/reductase, a carboxylating enoyl-thioester reductase** *Proc. Natl. Acad. Sci.* **106,** 8871–8876 (2009).

79. Mansell, D. J., Toogook, H. S., Waller, J., Hughes, J. M. X., Levy, C. W., Gardiner, J. M. and Scrutton, N. S. **Biocatalytic asymmetric alkene reduction: crystal structure and characterization of a double bond reductase from *nicotiana tabacum*** *ACS Catal.* **3,** 370–379 (2013).

80. Wilkins, A. D., Bachman, B. J., Erdin, S. and Lichtarge, O. **The use of evolutionary patterns in protein annotation** *Curr. Opin. Struct. Biol.* **22,** 316–325 (2012).

81. Porté, S., Valencia, E., Yakovtseva, E. A., Borràs, E., Shafqat, N., Debreczeny, J. E., Pike, A. C., Oppermann, U., Farrés, J., Fita, I. and Parés, X. **Three-dimensional structure and enzymatic function of proapoptotic human p53-inducible quinone oxidoreductase PIG3** *J. Biol. Chem.* **284,** 17194–17205 (2009)

82. Thorn, A., Egerer-Sieber, C., Jäger, C. M., Herl, V., Müller-Uri, F., Kreis, W. and Muller, Y. A. **The crystal structure of progesterone 5beta-reductase from Digitalis lanata defines a novel class of short chain dehydrogenases/reductases** *J. Biol. Chem.* **283,** 17260–17269 (2008).

83. Pinzar, E., Miyano, M., Kanaoka, Y., Urade, Y. and Hayaishi, O. **Structural basis of hematopoietic prostaglandin D synthase activity elucidated by site-directed mutagenesis** *J. Biol. Chem.* **275,** 31239–31244 (2000).

84. Chang, C. S., Negishi, M., Nishigaki, N. and Ichikawa, A. **Characterization of functional interaction of carboxylic acid group of agonists and arginine of the seventh transmembrane domains of four prostaglandin E receptor subtypes** *Prostaglandins* **54,** 437–446 (1997).

85. Cao, H., Yu, R., Tao, Y., Nikolic, D. and van Breemen, R. B. **Measurement of cyclooxygenase inhibition using liquid chromatography-tandem mass spectrometry** *J. Pharm. Biomed. Anal.* **54,** 230–235 (2011).

86. Barnett, J., Chow, J., Ives, D., Chiou, M., Mackenzie, R., Osen, E., Nguyen, B., Tsing, S., Bach, C., Freire, J., et al. **Purification, characterization and selective inhibition of human prostaglandin G/H synthase 1 and 2 expressed in the baculovirus system** *Biochi.m Biophys. Acta.* **1209,** 130-139 (1994).